

Supporting Information

Systematic Extension of the Length of the Organic Conjugated π -System of Mesoporous Silica-based Organic-Inorganic Hybrid Materials

Maximilian Cornelius, Frank Hoffmann, Boris Ufer, Peter Behrens and Michael Fröba*

Characterisation of the new organosilane precursors:

Characterisation of the organosilane precursor 4,4'-bis-((*E*)-2-(triethoxysilyl)vinyl)stilbene (BTEVS)

^1H NMR:

^1H NMR (CDCl_3 , 200 MHz): δ 1.28 (*t*, 18 H, $J = 7.0$ Hz), 3.89 (*q*, 12 H, $J = 7.0$ Hz), 6.19 (*d*, 2 H, $J = 19.3$ Hz), 7.1 (*s*, 2 H), 7.22 (*d*, 2 H, $J = 19.3$ Hz), 7.48 (*s*, 8 H);

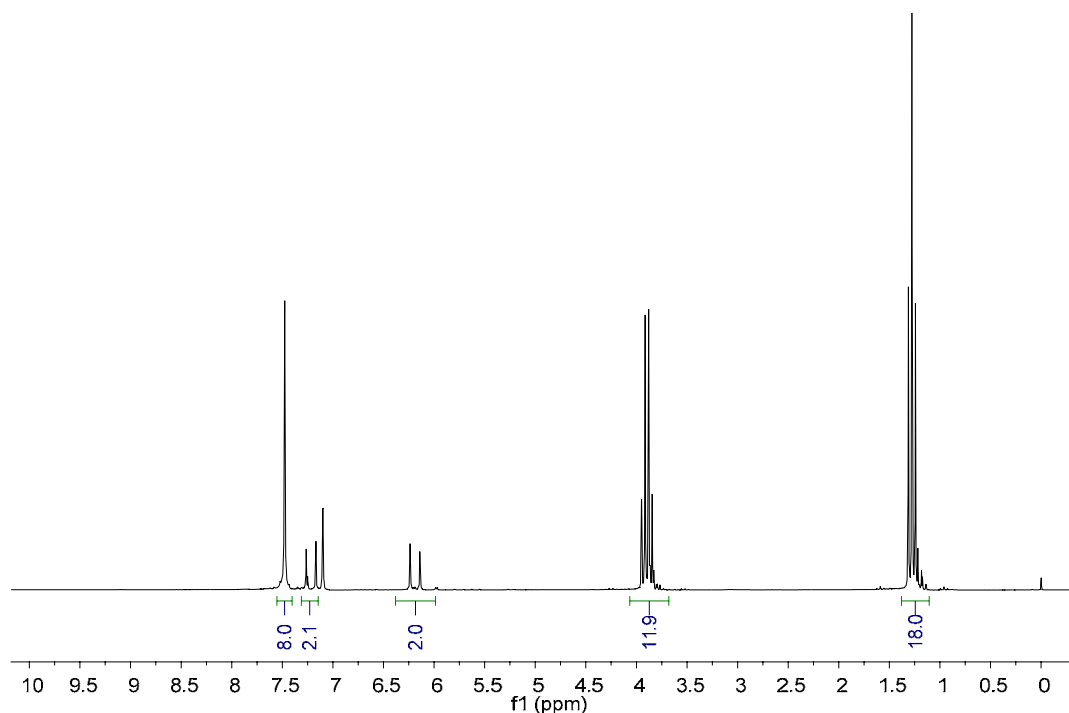


Figure S1. ^1H NMR spectrum of 4,4'-bis-((*E*)-2-(triethoxysilyl)vinyl)stilbene measured in CDCl_3 .

$^{13}\text{C} \{^1\text{H}\}$ NMR:

$^{13}\text{C} \{^1\text{H}\}$ NMR (CDCl_3 , 100 MHz): δ 18.4 ($\text{CH}_3\text{-CH}_2$), 58.7 ($\text{CH}_3\text{-CH}_2$), 117.7 (CH-Si), 126.8 ($\text{C}_{\text{arom.H}}$), 127.2 ($\text{C}_{\text{arom.H}}$), 128.6 ($\text{CH-C}_{\text{arom.}}$), 137.0 ($\text{C}_{\text{arom.}}$), 137.7 ($\text{C}_{\text{arom.}}$), 148.6 ($\text{CH-C}_{\text{arom.}}$);

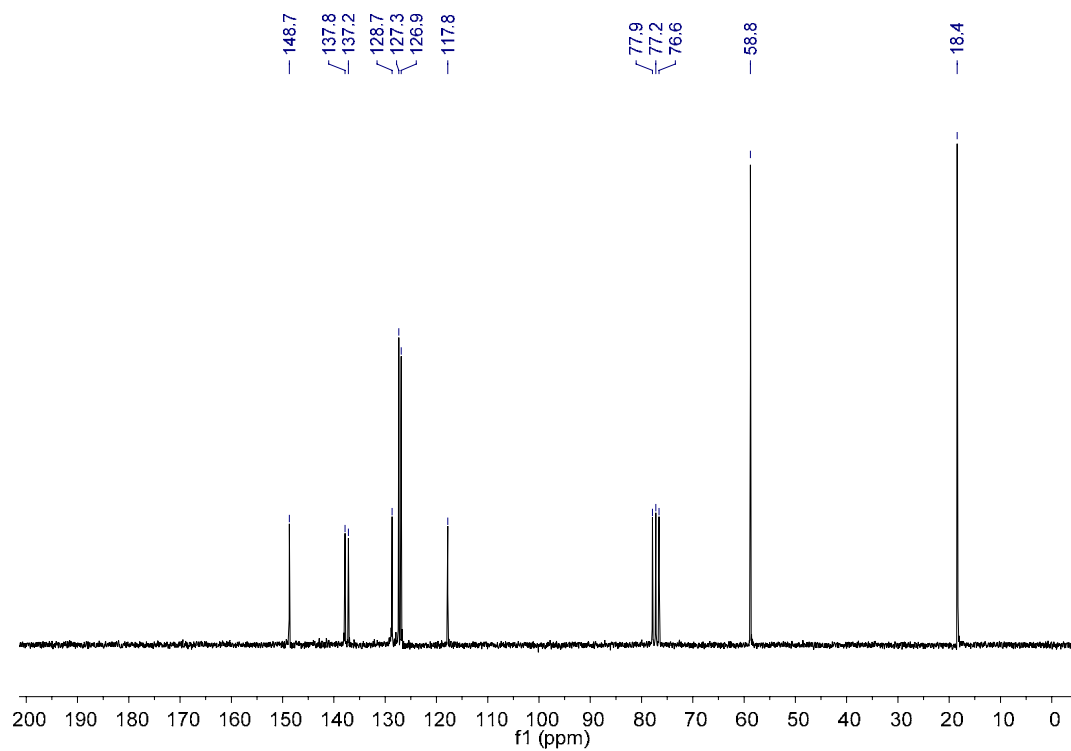


Figure S2. $^{13}\text{C} \{^1\text{H}\}$ NMR spectrum of 4,4'-bis-((*E*)-2-(triethoxysilyl)vinyl)stilbene measured in CDCl_3 .

FT-IR:

FT-IR (film, cm^{-1}): 2975, 2926, 2887, 1602, 1513, 1390, 1166, 1102, 1079, 962, 827, 802

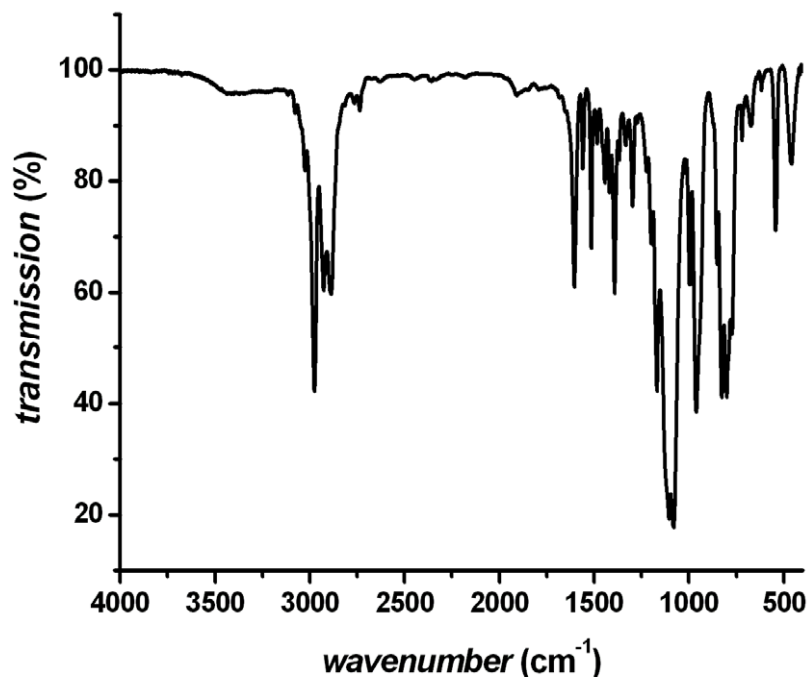


Figure S3. FT-IR spectrum of 4,4'-bis-((*E*)-2-(triethoxysilyl)vinyl)stilbene measured as film.

Characterisation of the organosilane precursor 4,4'-bis-((*E*)-2-(triethoxysilyl)vinyl)diazene (BTEVAB)

¹H-NMR:

¹H-NMR (CDCl₃, 200 MHz) δ (ppm) = 1,16 (*t*, 18 H, $J = 7,0$ Hz, CH₂-CH₃); 3,79 (*q*, 12 H, $J = 7,0$ Hz, O-CH₂); 6,18 (*d*, 2 H, $J = 19,3$ Hz, CH=CH-Si); 7,16 (*d*, 2 H, $J = 19,3$ Hz, CH=CH-Si); 7,48 (*m*, 4 H, CH=CH-C_{arom.}-C_{arom.}-H); 7,79 (*m*, 4 H, N=N-C_{arom.}-C_{arom.}-H)

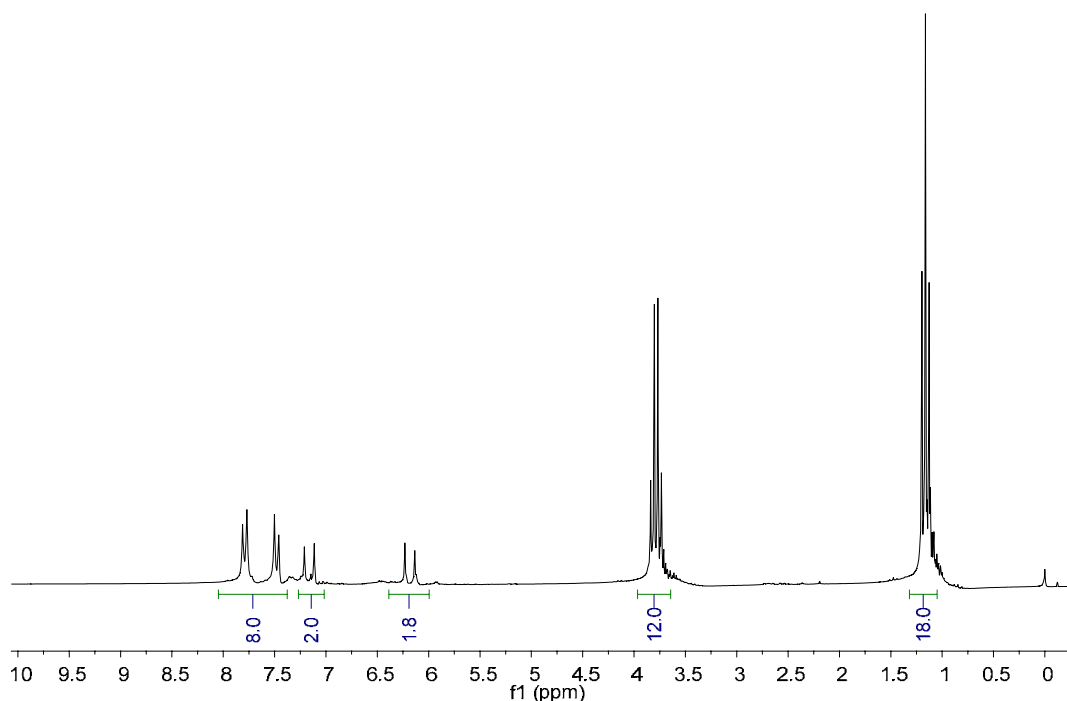


Figure S4. ¹H NMR spectrum of 4,4'-bis-((*E*)-2-(triethoxysilyl)vinyl)diazene measured in CDCl₃.

$^{13}\text{C} \{^1\text{H}\}$ -NMR:

$^{13}\text{C} \{^1\text{H}\}$ -NMR (CDCl_3 , 50 MHz) δ (ppm) = 17,9 ($\text{CH}_2\text{-CH}_3$); 58,2 (O-CH_2); 119,8 (Si-CH);
123,2 (CH=CH-Si); 127,2 ($\text{N=N-C}_{\text{arom.}}\text{-C}_{\text{arom.}}\text{-H}$); 139,7 ($\text{CH=CH-C}_{\text{arom.}}\text{-C}_{\text{arom.}}\text{-H}$); 147,8
($\text{C}_{\text{arom.}}\text{-CH=CH}$); 152,2 ($\text{C}_{\text{arom.}}\text{-N=N}$)

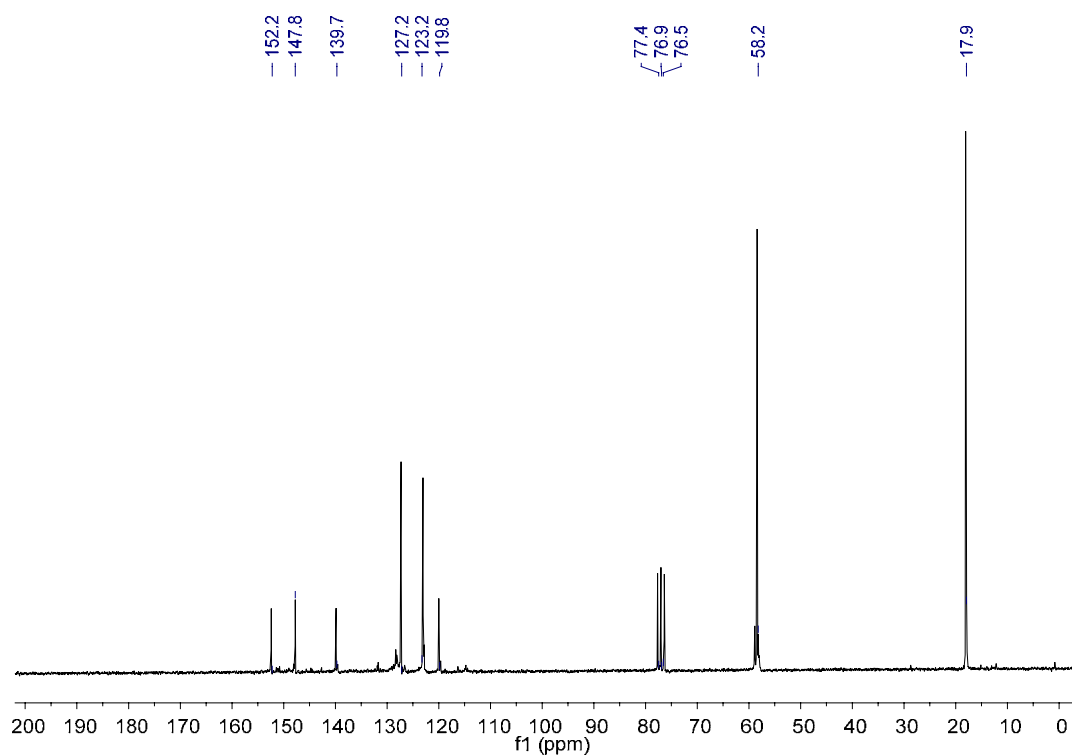


Figure S5. $^{13}\text{C} \{^1\text{H}\}$ NMR spectrum of 4,4'-bis-((*E*)-2-(triethoxysilyl)vinyl)diazene measured in CDCl_3 .

FT-IR:

FT-IR (Film, cm^{-1}): 2973, 2925, 2886, 1600, 1390, 1166, 1101, 1078, 959, 805

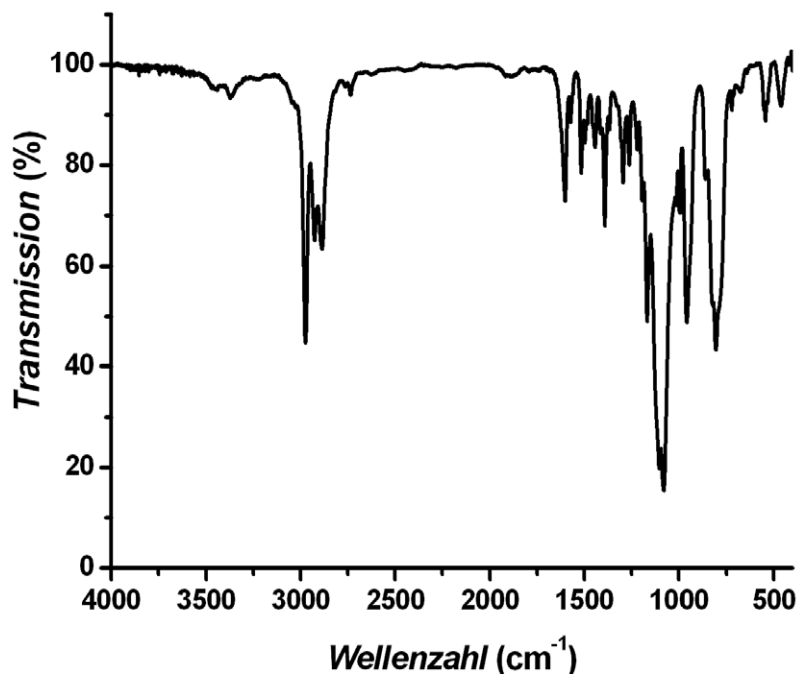


Figure S6. FT-IR spectrum of 4,4'-bis-((*E*)-2-(triethoxysilyl)vinyl)diazene measured as film.

Characterisation of the mesoporous hybrid materials

Ethene-bridged hybrid material (1):

The powder X-ray diffraction pattern of the mesoporous ethene-bridged hybrid material reveals only one reflection at $2.05^\circ 2\theta$ ($d = 4.31$ nm), indicating a periodic arrangement of the mesopores. The lack of further reflections in the wide-angle region indicates no crystal-like arrangement of the organic spacers within the pore walls.

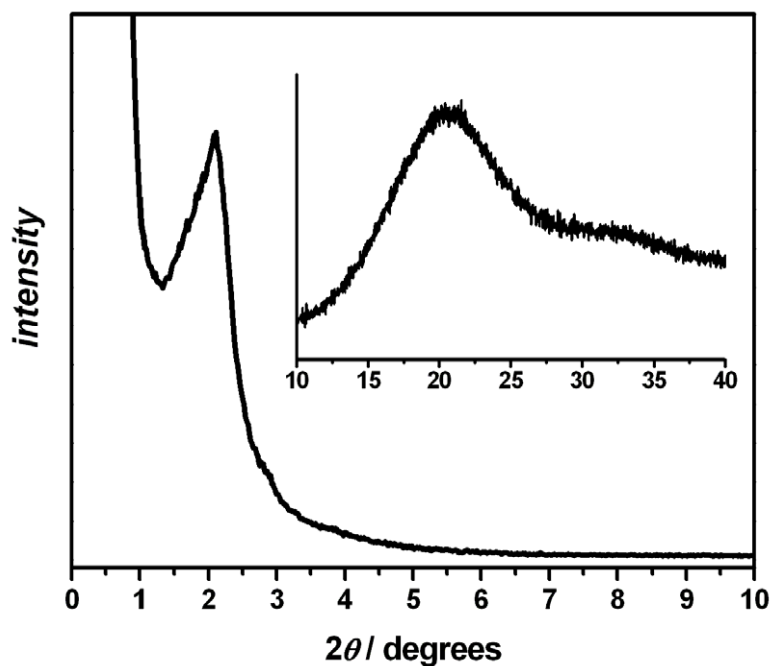


Figure S7. Powder X-ray diffraction pattern of the mesoporous ethene-bridged hybrid material.

Benzene-bridged hybrid material (2):

The powder X-ray diffraction pattern of the mesoporous benzene-bridged hybrid material reveals at least one sharp reflection at $2.02^\circ 2\theta$ ($d = 4.37$ nm), indicating a periodic arrangement of the mesopores. In addition three peaks at $2\theta = 11.59^\circ$ ($d = 0.76$ nm), 23.26° (0.38 nm), 35.39° (0.25 nm), which can be attributed to a crystal-like arrangement of the organic spacers within the pore walls.

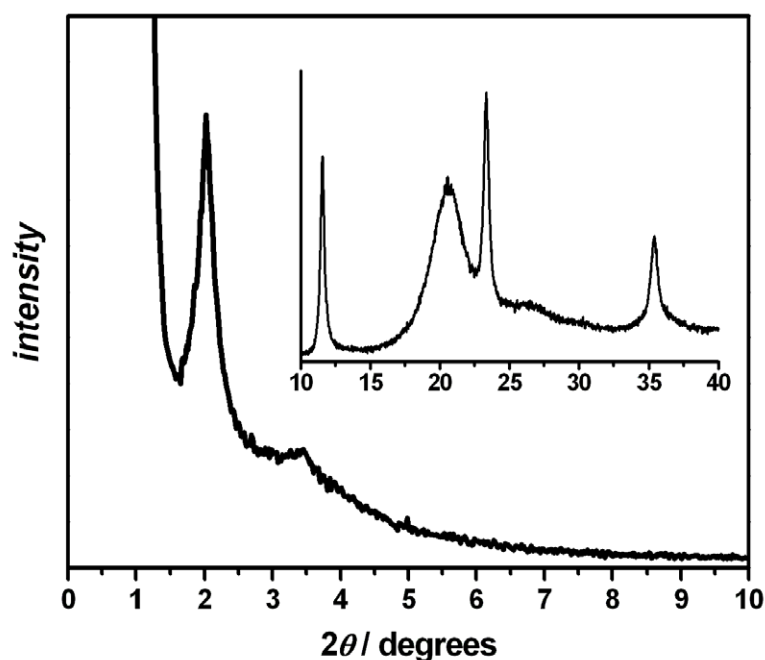


Figure S8. Powder X-ray diffraction pattern of the mesoporous benzene-bridged hybrid material.

The nitrogen physisorption measurement shows a type IV isotherm with a capillary condensation step at $p/p^0 = 0.3$. The mean pore diameter and the pore volume, as determined from the desorption branch by the BJH method, are 2.7 nm and $0.56 \times 10^{-6} \text{ m}^3/\text{g}$, respectively. The specific surface area determined by the BET method is $760 \text{ m}^2/\text{g}$.

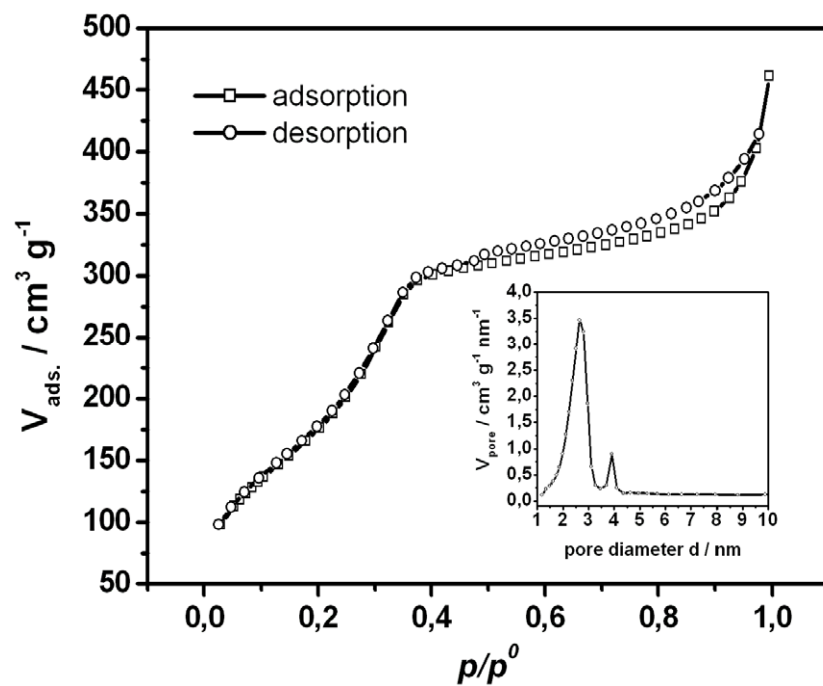


Figure S9. N_2 -physorption measurement of the mesoporous benzene-bridged PMO material measured at 77 K.

1,4-divinylbenzene-bridged hybrid material (3):

The powder X-ray diffraction pattern of the mesoporous 1,4-divinylbenzene-bridged hybrid material reveals one sharp reflection at $1.87^\circ 2\theta$ ($d = 4.72$ nm), indicating a periodic arrangement of the mesopores. In addition five peaks at $2\theta = 7.42^\circ$ ($d = 1.19$ nm), 14.78° (0.60 nm), 22.17° (0.40 nm), 29.82° (0.30 nm), 37.42° (0.24 nm) which can be attributed to a crystal-like arrangement of the organic spacers within the pore walls.

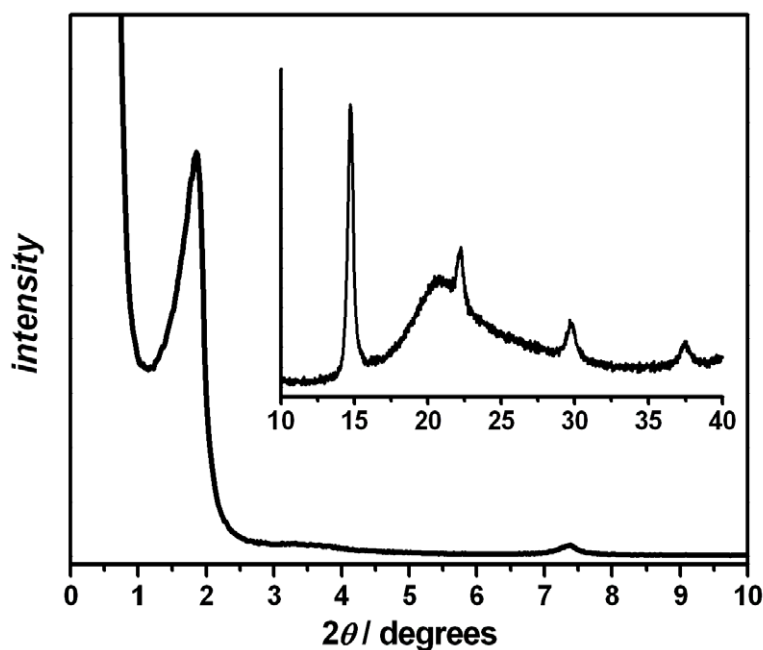


Figure S10. Powder X-ray diffraction pattern of the mesoporous 1,4-divinylbenzene-bridged hybrid material.

The nitrogen physisorption measurement shows a type IV isotherm with a capillary condensation step at $p/p^0 = 0.35$. The mean pore diameter and the pore volume, as determined from the desorption branch by the BJH method, are 2.8 nm and $0.62 \times 10^{-6} \text{ m}^3/\text{g}$, respectively. The specific surface area determined by the BET method is $794 \text{ m}^2/\text{g}$.

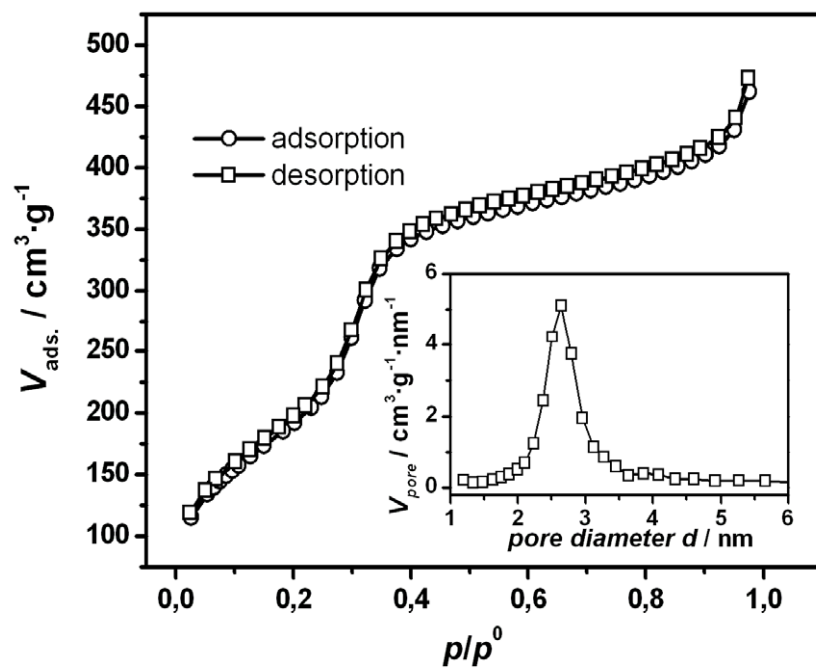


Figure S11. N₂-physorption measurement of the mesoporous 1,4-divinylbenzene-bridged PMO material measured at 77 K.

²⁹Si MAS NMR

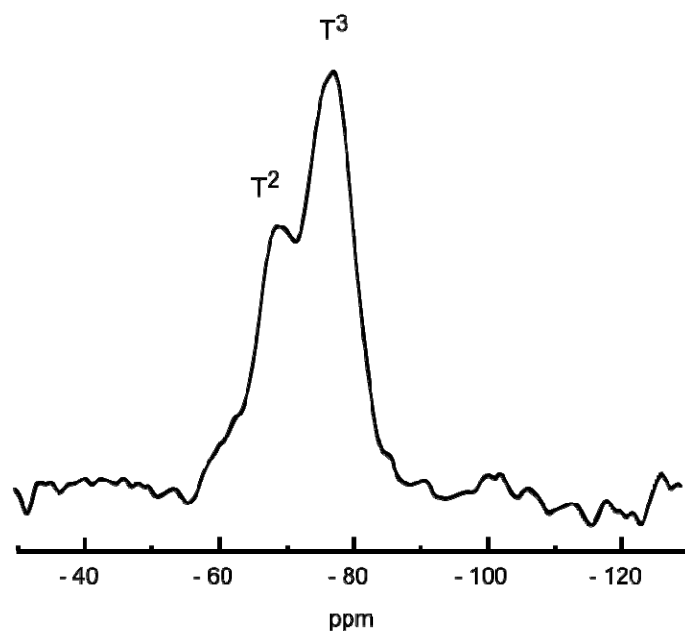


Figure S12. ²⁹Si MAS NMR spectrum of the mesoporous 4,4'-divinylstilbene-bridged hybrid material.

Transmission electron microscopy:

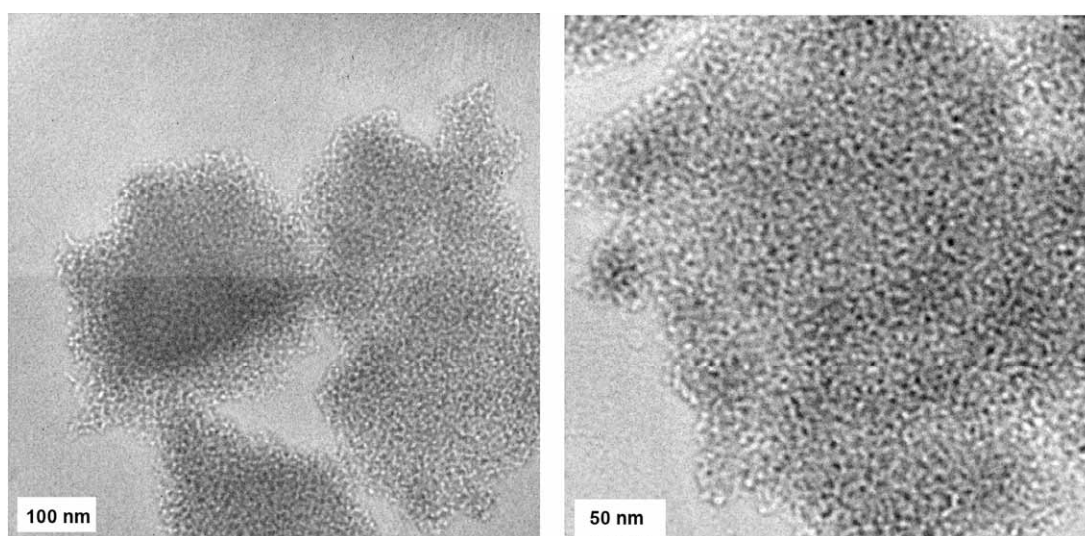


Figure S13. TEM images of the mesoporous 4,4'-divinylstilbene-bridged hybrid material.

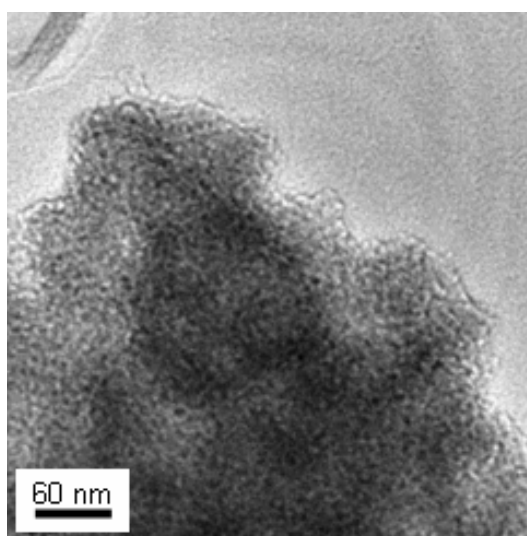


Figure S14. TEM image of the mesoporous 4,4'-divinylazobenzene-bridged hybrid material